Supporting Information

Manipulating Phonon Polaritons in Low Loss ^{11}B enriched Hexagonal Boron Nitride with Polarization Control

Lu Wang,[a, b] Runkun Chen,[a, b] Mengfei Xue,[a, b] Song Liu,[c] James H. Edgar[c] and Jianing Chen*[a, b, d]

[a]The Institute of Physics, Chinese Academy of Sciences, P.O. Box 603, Beijing, 100190, China. E-mail: jnchen@iphy.ac.cn.

[b]School of Physical Sciences, University of Chinese Academy of Sciences, Beijing 100049, China

[c] Tim Taylor Department of Chemical Engineering, Kansas State University, Manhattan, KS 66506, USA

[d]Songshan Lake Materials Laboratory Dongguan, 523808 Guangdong, China

Materials and Methods:

Sample preparation: Microcrystals of hBN were mechanically exfoliated from bulk samples and then transferred to 300-nm-thick SiO_2/Si substrate, and the ^{11}B isotope-enriched hBN crystals were grown by the metal flux technique[1].

Experimental Setup: The s-SNOM is a commercial system (Neaspec GmbH) equipped with QCLs (from Daylight Solutions). The incident frequency from 1500 to 1600 cm^{-1}. The s-SNOM is based on an AFM (its curvature radius is about 20nm), work at 280 kHz in the tapping mode and an amplitude of ~100 nm.

Nano-FTIR Measurements: Infrared reflectance measurements were performed using a FTIR spectrometer module based on the s-SNOM.

Raman Measurements: Raman measurements were performed using the 532 nm laser line of an argon-ion laser within a Renishaw Raman microscope. The power of laser line is 5mw, the scattered light was dispersed using an 1800 groove/mm grating onto a CCD.

Numerical Simulations: Numerical simulations were conducted by the commercial software package Comsol in 3D Wave Optics Module, which is based on finite element method. In the simulation model, the Natural hBN was set to 80 nm thickness, and the 99.2% ^{11}B hBN was set to 84 nm thickness corresponding to the experimental data, and the hBN film was put on a SiO_2 substrate. Then an *s*-polarized plane wave as a background field was set to replace the laser to illuminate the edge of hBN, and the boundary of the model was set as scattering and periodic boundary conditions. The simulated vertical component of electric field E_z above 5 nm of the hBN was recorded to compare with the experimental edge-excited HPPs. The minimum mesh size was set to 1 nm to achieve a good convergent result. The permittivities of the SiO_2 substrate and hBN were obtained from the previous reported [2,3].

Supplemental experiments and simulations:

1. Topography and line profiles of hBN samples

The topography of hBN samples (Natural and isotope-enriched) were characterized by Atom Force Microscopy integrated on the s-SNOM.

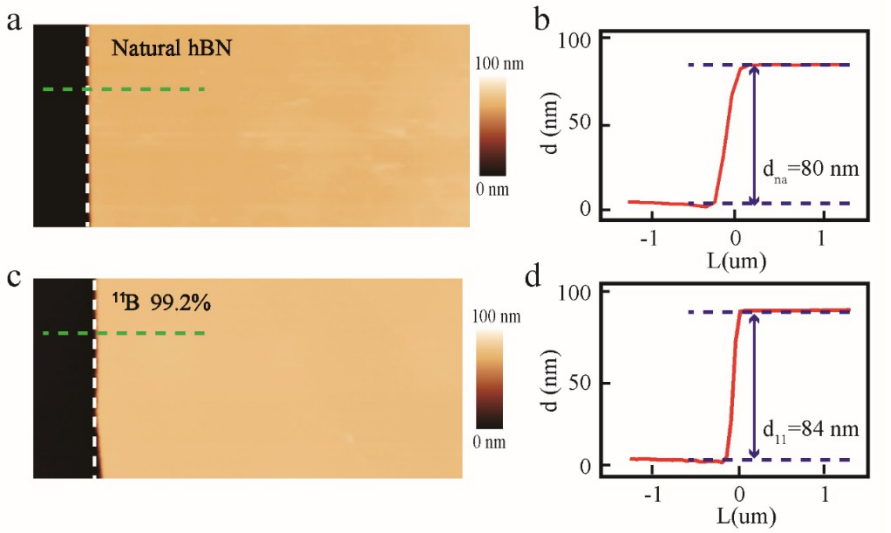

Figure S1. The topography of hBN samples. (a) and (c): AFM topography imaging of Natural hBN and 99.2% ^{11}B hBN. White dashed line at L=0 marks the edge of hBN crystal. (b) and (d): Line profiles taken perpendicular to Natural and 99.2% ^{11}B hBN edge (along green dashed line in (a) and (c).

2. Raman spectra of hBN samples

Raman spectra were used to characterize the varying isotopic purity of hBN[3]. The Spectra of the two hBN samples are shown in Figure S2.

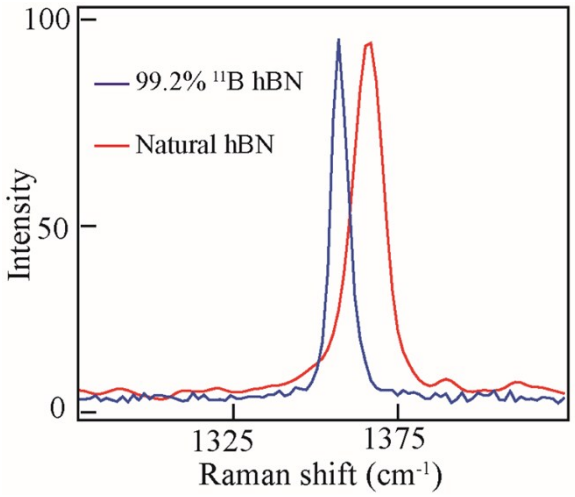

Figure S2. 532 nm Raman spectra of Natural and 99.2% ^{11}B hBN. The red line is from the Natural hBN Raman spectra, the blue line from the 99.2% ^{11}B hBN Raman spectra, a clear spectral shift and reduction in linewidth.

3. Permittivities of hBN samples

The permittivity of hBN (Natural and 99.2% ^{11}B hBN) was described by the Lorentz model[3-5]:

$$\varepsilon_i(\omega) = \varepsilon_\infty\left(1 + \frac{(\omega_{LO,i})^2 - (\omega_{TO,i})^2}{(\omega_{TO,i})^2 - \omega^2 - i\omega\gamma_i}\right), i = t,z$$

Where the i= t (z) represents the in-plane (out-of-plane) permittivity perpendicular (parallel) to the c axes; ω, ω_{LO}, ω_{TO}, γ and ε_∞ represent the incident frequency, the LO and TO phonon frequency, the phonon damping rate and high-frequency permittivity. In this work, these parameters of Natural and 99.2% ^{11}B hBN are taken from the previous reference. The real part of the permittivities of Natural and 99.2% ^{11}B hBN are shown in Figure S3.

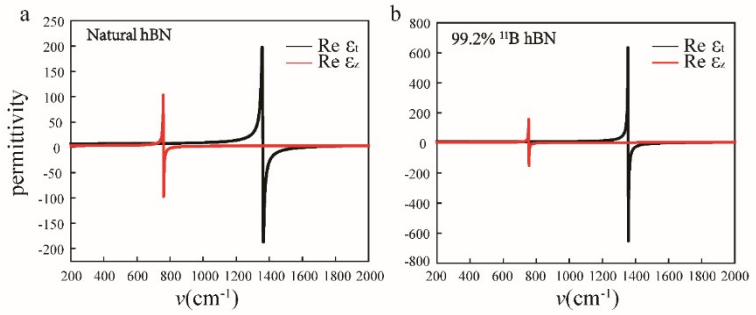

Figure S3. Real part of the in-plane and out-of-plane permittivities of Natural and 99.2% ^{11}B hBN.

4. The FOM and propagation lengths of HPPs with different upper band phonon damping rates

The theoretical calculation of figure of merit (FOM) and propagation length of HPPs don't consider the experimental loss and similar deviations can be found in the other work [3]. We add an extra calculation with a phonon damping rate of 3.5 cm^{-1}, and the calculated result shows a good agreement with the experimental data. However, considering the experiment loss, the damping rate may be smaller than 3.5 cm^{-1}. The origin and the mechanism of damping are not in the scope of this paper. Therefore, according to the fittings, the actual phonon damping rate in 99.2% ^{11}B hBN is greater than the theoretical result of 2.1 cm^{-1} and smaller than 3.5 cm^{-1}.

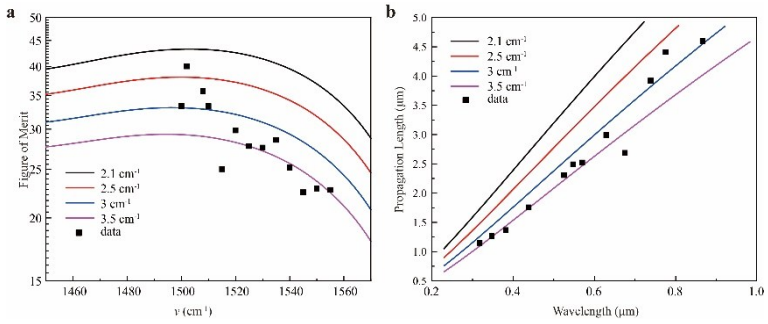

Figure S4. The FOM (a) and propagation length (b) of HPPs in 99.2% ^{11}B hBN with different upper band phonon damping rates.

5. HPPs Near field imaging at different polarized angles

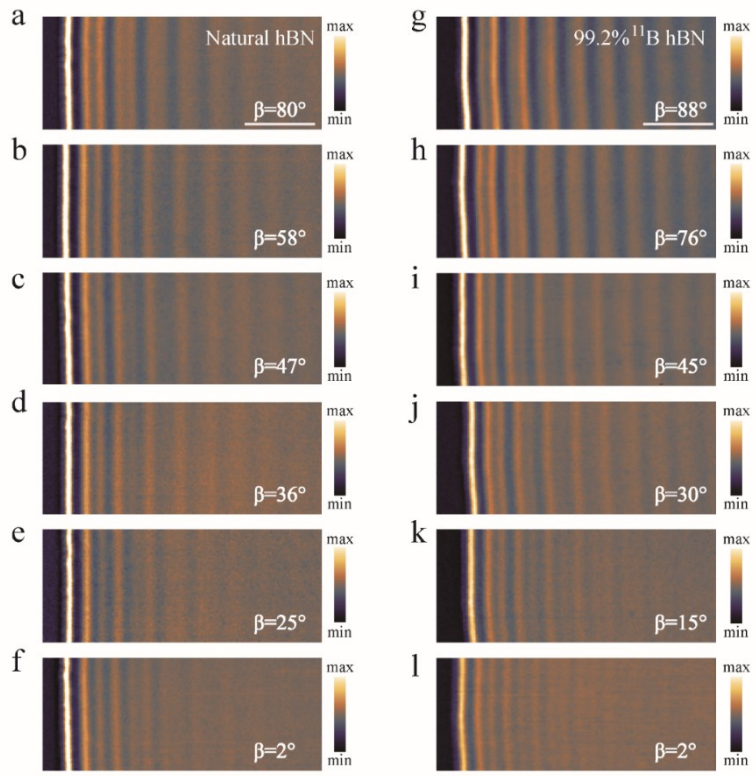

Figure S5. Real space imaging of HPPs in hBN at different *s*-polarized angles incident light. (a)-(f) Real space imaging of HPPs in Natural hBN at an *s*-polarized angle of 80°, 58°, 47°, 36°, 25° and 2°. (g)-(l) Real space imaging of HPPs in 99.2% ^{11}B hBN at an *s*-polarized angles of 88°, 76°, 45°, 30°, 15° and 2°. The scale bar is 2 um.

6. Simulated electric field intensity of HPPs at different angles

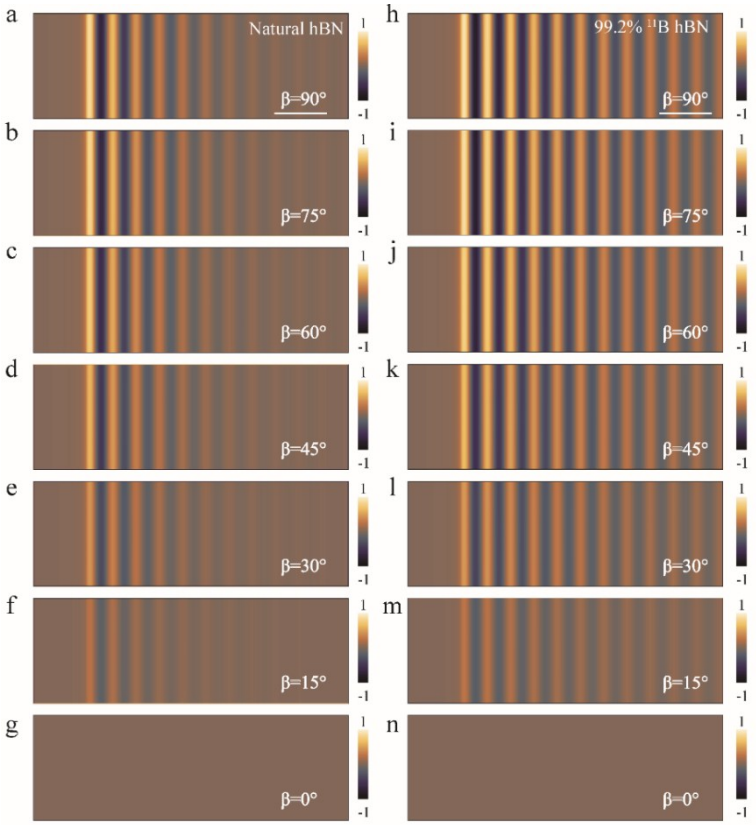

Figure S6. Simulation of the edge-excited electric field E_z of HPPs in hBN with different *s*-polarization angle β. (a)-(g) Edge-excited electric field E_z of HPPs in Natural hBN with different *s*-polarized angle β. (h)-(n) Edge-excited electric field E_z of HPPs in 99.2% ^{11}B hBN with different *s*-polarized angle β. The scale bar is 2 um.

7. Simulated angularly dependent edge excitation normalized NEFI of HPPs

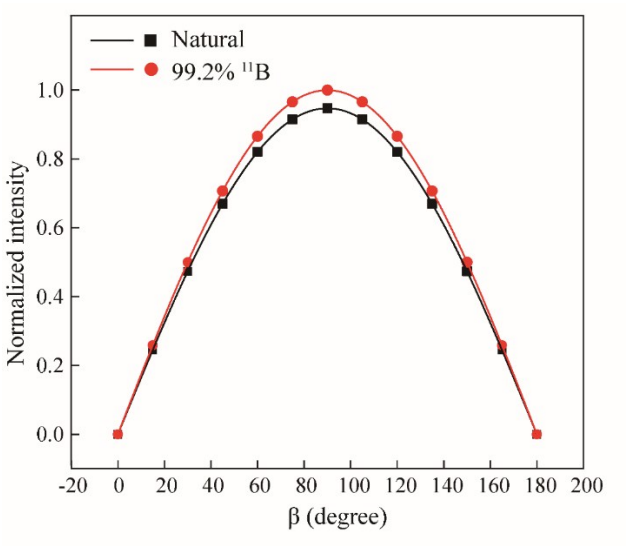

Figure S7. Simulated angularly dependent edge excitation normalized NEFI of HPPs in Natural and 99.2% ^{11}B hBN. The black square and red dot represent the simulation results for Natural and 99.2% ^{11}B hBN, and the black and red solid line represent the sine fitting result.

References:

1. S. Liu, R. He, L. Xue, J. Li, B. Liu, and J.H. Edgar, Chem. Mater. 30 6222-6225
2. Z. Fei, G. O. Andreev, W. Bao, L. M. Zhang, A. S. McLeod, C. Wang, M. K. Stewart, Z. Zhao, G. Dominguez and M. J. N. l. Thiemens, 2011, **11**, 4701-4705.
3. A. J. Giles, S. Y. Dai, I. Vurgaftman, T. H. Man, S. Liu, L. Lindsay, C. T. Ellis, N. Assefa, I. Chatzakis, T. L. Reinecke, J. G. Tischler, M. M. Fogler, J. H. Edgar, D. N. Basov and J. D. Caldwell, *Nat Mater*, 2018, **17**, 134-+.
4. P. N. Li, M. Lewin, A. V. Kretinin, J. D. Caldwell, K. S. Novoselov, T. Taniguchi, K. Watanabe, F. Gaussmann and T. Taubner, *Nat Commun*, 2015, **6**.
5. E. Yoxall, M. Schnell, A. Y. Nikitin, O. Txoperena, A. Woessner, M. B. Lundeberg, F. Casanova, L. E. Hueso, F. H. L. Koppens and R. Hillenbrand, Nat Photonics, 2015, 9, 674-+.